Available online at www.sciencedirect.com
SCIENCE DIRECT®
Catalysis Today 99 (2005) 171–177
www.elsevier.com/locate/cattod

Vapour phase oxidation of toluene in V/Al_2O_3–TiO_2 catalytic reactors

A. Bottino[a], G. Capannelli[a,*], A. Comite[a], R. Di Felice[b]

[a]Dipartimento di Chimica e Chimica Industriale, Università degli Studi di Genova, via Dodecaneso 31, 16146 Genoa, Italy
[b]Dipartimento di Ingegneria Chimica e di Processo "G. Bonino", Università degli Studi di Genova,
via Opera Pia 15, 16145 Genoa, Italy

Abstract

The catalytic membrane reactor and the inert packed bed membrane reactor were studied in the vapour phase selective oxidation of toluene. Different feeding policies for the membrane were explored and their influence on the selectivity to the desired products (benzaldehyde and benzoic acid) was investigated. The active phase was prepared by depositing vanadium on a Al_2O_3–TiO_2 support prepared through the sol–gel technique. Higher selectivity to benzaldehyde was obtained using the catalytic membrane reactor. Differences were seen in the catalytic membrane reactor performance only when the active phase was heavily charged along the membrane cross-section.
© 2004 Elsevier B.V. All rights reserved.

Keywords: Toluene gas phase oxidation; Selective oxidation; Catalytic membrane reactor; Inert packed bed membrane reactor; Ceramic membrane

1. Introduction

While the gas phase partial oxidation of some alkylaromatics has become an industrial reality (e.g. *o*-xylene oxidised to maleic anhydride), the vapour phase selective oxidation of toluene with high yields of valuable intermediate products (e.g. benzaldehyde, benzoic acid, etc.) is still a challenge [1], the liquid phase route being industrially preferred [2,3]. For the catalysts studied until now, the contribution of combustion reactions (which form CO and CO_2) is very high. Among the various catalyst studied for the selective oxidation of toluene to useful products, the vanadium-based catalysts gave the best catalytic performance. Vanadium can be used as bulk V_2O_5 [4] or supported on a oxide like TiO_2 [5,6] with an eventual addition of other species (e.g. K or P) to enhance the selectivity [7–12]. The type of support is a key factor in the catalyst development for the selective oxidation of alkylaromatics [13,14].

The use of reactors different from the conventional packed bed reactor (PBR) to enhance the selectivity to useful products in the partial oxidation of toluene is still poorly investigated. Inorganic membrane reactors have been studied in several partial oxidation reactions in order to improve the selectivity to intermediate products [15–28] or to enhance the safety of the process by separating the stream of the oxidiser from that of the hydrocarbon [16,18,19,29].

The membrane itself can be catalytic (catalytic membrane reactor) or support a catalytic bed (inert membrane packed bed reactor). In the catalytic membrane reactor (CMR), the catalytic phase can be arranged as a thin layer or impregnated in the tube porous structure.

In this work, the catalytic performance of the V/Al_2O_3–TiO_2 implemented as inorganic membrane reactors was investigated for the vapour phase selective oxidation of toluene. In a previous paper [30] the kinetic parameters for the oxidation of toluene over a V/Al_2O_3–TiO_2 catalyst were estimated and on the basis of the calculated selectivity-conversion trends a comparison between the PBR and the CMR was made. It was shown that efficiency factor of the CMR depends on the vanadium content and distribution along the membrane cross-section. This paper gives further data on the characterisation and use of ceramic membranes as CMR and IMPBR, moreover the influence of the feeding

---

* Corresponding author. Tel.: +39 010 3536197; fax: +39 010 3536199.
E-mail address: capannel@unige.it (G. Capannelli).

0920-5861/$ – see front matter © 2004 Elsevier B.V. All rights reserved.
doi:10.1016/j.cattod.2004.09.037

configurations (co-feed and separate feed modes) on the products selectivity was experimentally studied.

2. Experimental

2.1. Preparation of the V/Al_2O_3–TiO_2 catalyst as a powder or a catalytic membrane reactor

The mixed Al_2O_3–TiO_2 oxide was prepared using the sol–gel technique. The boehmite (about 0.7 M as Al) and the titania (about 0.2 M as Ti) sols were prepared via acid catalysed hydrolysis of the respective alkoxides. The two sols were then mixed in order to give a single sol with a equal molar content of aluminium and titanium.

To obtain a powdered Al_2O_3–TiO_2 oxide, the mixed Al–Ti-based sol was dried in a Petri dish. The xerogel was then ground and sieved collecting the 80–150 μm fraction. It was finally calcined at 400 °C in an air stream.

Two catalytic membranes were prepared from the same Al–Ti-based sol after adding 0.34% (w/w) of hydroxipropylcellulose to prevent the formation of drying-stress defects in the final top-layer. The first membrane, hereafter called the ATV membrane, was prepared using the dip-coating method as described in [31]. The ceramic tube used (Atech, Germany) had an asymmetrical porous structure with a 0.2 μm nominal pore diameter on the surface of the internal side. The coating procedure was carried out by filling the internal side of the ceramic tube with the mixed sol for 4 s.

The second catalytic membrane, called ATVimp membrane, was obtained by letting the sol infiltrate twice into the porous structure of a ceramic tube (20 kD supplied by Atech, Germany). The infiltration apparatus consisted of a water ejector connected to one end of the membrane, while the other end was closed. The tube was then dipped for 30 s in the sol, which under the driving force of the pressure difference, flowed from the external side towards the internal side of the membrane. The two membranes were dried at room temperature for 12 h and then calcined in air up to 400 °C.

Vanadium was deposited on both the powders and membranes using the equilibrium adsorption technique from an ammonium metavanadate water solution (250 mg/L, 24 h). The powders and the membranes after precursor deposition were calcined in air up to 400 °C.

2.2. SiO_2 membrane preparation

The SiO_2 membrane was prepared using the dip-coating technique from a commercial aqueous colloidal SiO_2 (40% (w/w)) sol (Ludox ASGI, Du Pont) [32,33]. An aqueous solution of polyvinylalcohol was added as a binder. The ceramic tube used was supplied by SCT US Filter and had a 0.2 μm nominal pore diameter in the inner layer. The tube was 15 cm long and was enamelled to 50 mm at both ends.

2.3. Characterisations

Specific surface areas and pore dimensions were determined by the BET and the DFT methods, respectively, using a Micromeritics ASAP 2010 instrument. The Raman spectra were recorded on a Renishaw 1000 instrument equipped with a Leika microscope and an Ar laser at 633 nm. The measurements were carried out in air.

The vanadium loading on the catalytic powder and catalytic membranes was first determined by dissolving a catalytic sample with HF and hot ‘‘aqua regia’’ (1 part of concentrated HNO_3 and 3 parts of concentrated HCl) and then through flame atomic absorption spectroscopy (AAS, Varian SPECTRAA 55B).

The surface morphology and cross-section structure of the membranes along with the element location of vanadium, were analysed using a Leo Stereoscan scanning electron microscope (SEM) equipped with an EDX (Ge probe Link Oxford) and a back scattering probe (Centaurus, Oxford).

The transmission electron microscope (TEM, Jeol Jem-2010, with EDS detector, Oxford–Link Pentafet) was used to observe the eventual presence of vanadium oxide crystallites.

Permeation measurements were carried out at room temperature using pure nitrogen or helium. One of the ends of the membrane was closed so that the gas flowed through the membrane area from the lumen to the external side of the tube. For each fixed flow rate the trans-membrane pressure and entry pressure were measured. In this way defects in the membrane preparation process were highlighted by both high permeance values and a high contribution of the laminar flow regime.

2.4. Catalytic tests

The rig is composed of a gas supply apparatus, the reactor and the analytical system. All the gases came from containers (supplied with a purity of 99.99% by Siad, Italy) and were regulated through mass flow controllers (Brooks Instruments). Toluene was passed to the vapour phase by flowing part of the inert gas (He) through a bubbling contactor. The total flow rate was set between 60 and 80 cm^3_{STP}/min. Toluene concentration in the feed mixture ranged from 0.2 to 0.5 mol%. The O_2–toluene molar ratio (O_2/T) was varied from 5 to 22. All the reactors worked isothermally and the temperature was kept constant by an electrical oven (mod. CTF, Carbolite).

A brief description of the reactors used is given below.

(I) The packed bed reactor was made of a quartz tube with an internal diameter of 12 mm. The catalytic powder (0.1110 g) was diluted with inert SiC (400 mesh, Aldrich) in a ratio of 10. A thin thermocouple was inserted in the middle of the catalytic bed.

(II) The catalytic membranes (ATV or ATVimp) were placed in a stainless steel housing designed to allow for

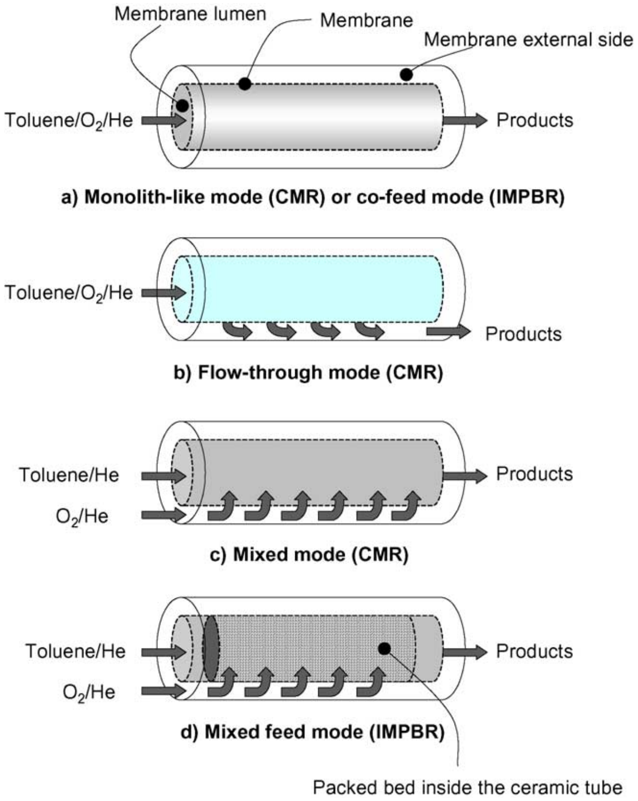

Fig. 1. Feeding modes used in the catalytic membrane reactors (monolith-like, flow through and mixed modes) and in the inert packed bed membrane reactor (co-feed mode and mixed-feed mode).

different feeding configurations. The gastight between the internal and external side of the membrane was assured through graphite gaskets. During the experiments, the reactor was fed in three different ways: monolith-like mode (Fig. 1a, toluene, O_2 and helium flow tangentially to the membrane surface in the internal side of the ceramic tube), flow-through mode (Fig. 1b, all the reactants were fed in the internal side of the membrane and were forced through the membrane surface while the other internal side outlet was closed) and the mixed mode (Fig. 1c, toluene and helium were fed inside the ceramic tube while oxygen was externally fed to the membrane. The reaction products and the unconverted reactants left the reactor from the internal side outlet).

(III) The inorganic membrane reactor was assembled in the same stainless housing used for the catalytic membrane reactor. The SiO_2 membrane contained a bed of the same powder catalyst used in the packed bed reactor. In this case, a higher catalyst dilution with inert carborundum (2.33 g of SiC and 0.155 g of catalyst) was used to obtain a catalytic bed with a sufficient length to completely fill the permeable part of the ceramic membrane. The performance of the inorganic membrane reactor was exploited using two configurations: co-feed (like the CMR shown in Fig. 1a, toluene, O_2 and helium were fed premixed to the packed bed contained inside the inert ceramic tube) and mixed-feed (Fig. 1d, toluene and helium were fed directly on the catalytic bed while oxygen was supplied through the membrane wall).

The line from the reactor exit to the gas sampling point was heated to 150 °C, to prevent product condensation. The analytical system consisted of two gas chromatographs (-Perkin-Elmer Sigma 3B equipped with a TCD for analysing non condensable gases on a Carbosphere 80/100 mesh c-olumn and a Perkin-Elmer 8700 to analyse the organic c-ompounds by FID on a FFAP 10% column).

3. Results and discussion

3.1. Characterisations

The specific surface area of the $V/Al_2O_3–TiO_2$ powder was about 211 m^2/g. The surface area (normalised to the tube length in order to carry out better comparisons) of the starting ceramic tubes and the catalytic membrane are summarised in Table 1. The specific surface area of the catalytic powder was higher than other catalytic systems reported in literature for the selective oxidation of toluene. The surface area for the unit of tube length of the catalytic membranes (ATV and ATVimp) is noticeably higher than that of the original supports. This fact is due to the presence of the added catalytic phase, $V/Al_2O_3–TiO_2$. Fig. 2 shows the pore dimension distributions for the catalytic powder and membranes. The $V/Al_2O_3–TiO_2$ catalytic phase (powder or catalytic membrane) was mesoporous with a pore diameter of about 6 nm. The comparison of pore dimension distribution for the powder (Fig. 2a) and membranes (Fig. 2b and c) indicate that they had very similar textural characteristics.

The amount of vanadium in the catalytic $V/Al_2O_3–TiO_2$ powder is about 5.4% (w/w). Catalyst loading on the catalytic membranes is reported in Table 1. The ATVimp catalytic membrane had a greater amount of vanadium deposited because in its porous structure the total amount of $Al_2O_3–TiO_2$ was greater than in the ATV membrane.

Fig. 3 shows the SEM micrographs of the active catalytic $V/Al_2O_3–TiO_2$ coating in the inner side of the ATV membrane (a) along with its surface (b). The ATV

Table 1
Specific surface area and catalytic loading for the catalytic membranes

Membrane	SSA (m^2/cm)	Pore diameter (nm)	Specific V loading (mg/cm)	Total V loading (mg)
0.2 μm Atech	0.22	200[a]	–	–
ATV	0.48	6.8	0.035	0.42
20 kD Atech	0.29	13	–	–
ATVimp	1.45	6.6	0.07	0.83

SSA: specific surface area.
[a] Nominal value as reported by the supplier.

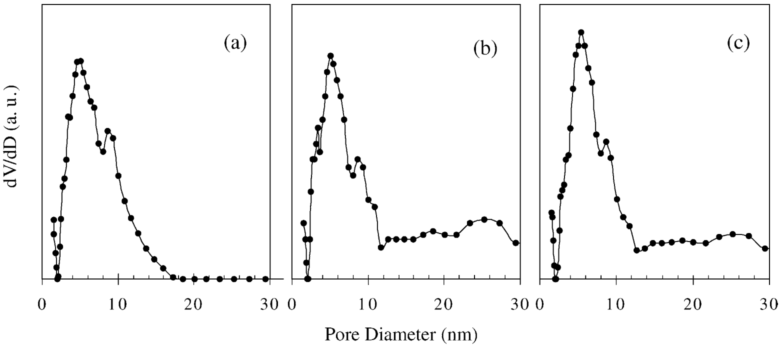

Fig. 2. Pore diameter distribution (BJH method applied to the adsorption branch) for the (a) V/Al_2O_3–TiO_2 powder, (b) ATV membrane and (c) ATVimp membrane.

membrane is formed of a very thin catalytic layer (about 2 μm), as can be seen in Fig. 3a. Neither vanadium nor presence of the titania–alumina support were found on the rest of the ceramic tube. The surface was defect-free and homogeneous (Fig. 3b).

The differences between the cross-section of the original ceramic tube and ATVimp were not easily visible by SEM. The sol nanoparticles were so small that they failed to fill the membrane pores. Instead, a very thin layer of sol formed on the grain surface (revealed by EDX analyses). Since in the more internal layers the exposed surface was greater (and the pore dimensions smaller), the titania–alumina concentration was higher than in the other zones. In other words, vanadium is present in the entire membrane cross-section the with a concentration profile growing from the outside to inside the tube.

Fig. 4 shows the Raman spectrum of the V/Al_2O_3–TiO_2 powder. The Raman lines at 643, 520, 408, 158 cm^{-1} can be assigned to the presence of the anatase phase. The frequency blushifts of about 10 cm^{-1} in the Raman bands, when compared to those of bulk anatase, are attributed to the smaller particle size of TiO_2 [34]. The weak bands of the

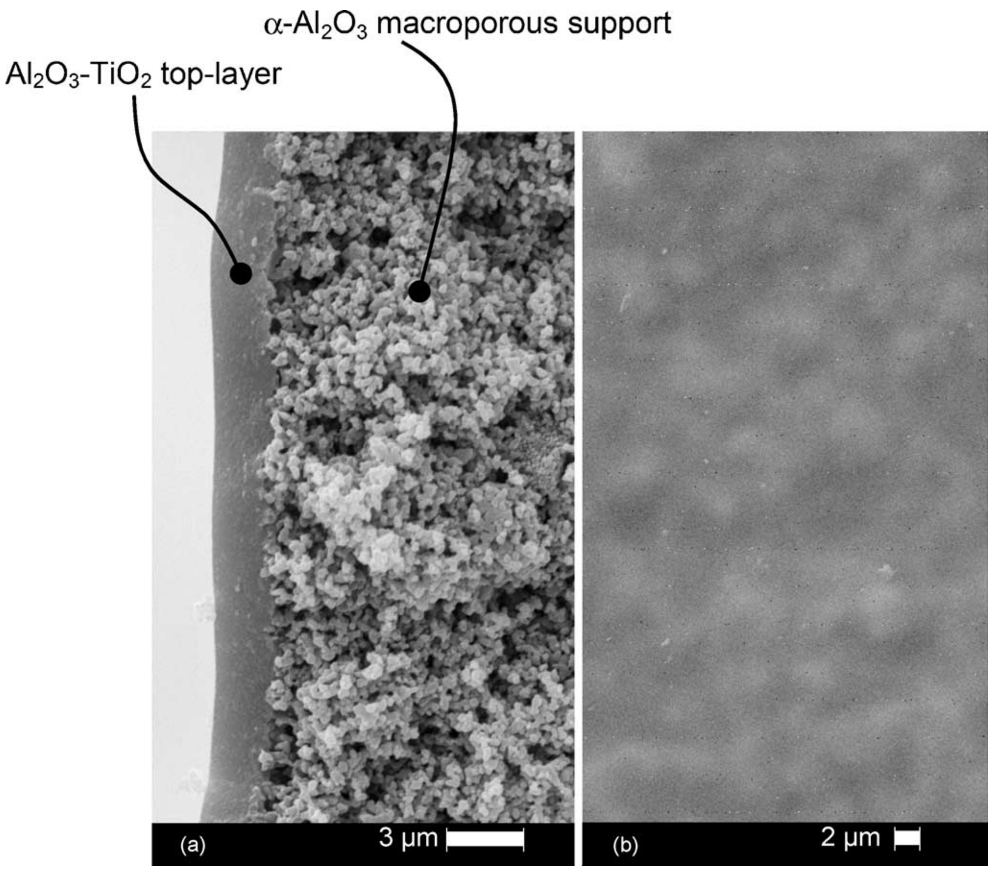

Fig. 3. SEM micrographs of the (a) cross-section and (b) surface of the ATV catalytic membrane.

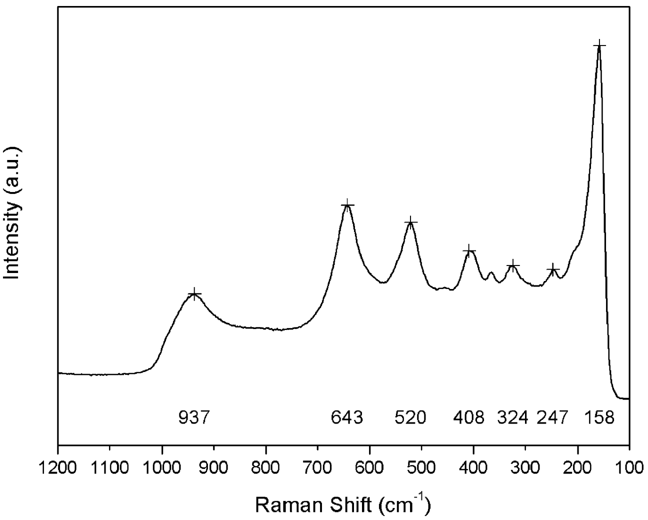

Fig. 4. Raman spectra of the V/Al_2O_3–TiO_2 powder.

brookite phase were at 363, 324, and 247 cm^{-1}. The typical bands of crystalline V_2O_5 (994, 694 and 530 cm^{-1}) were absent [35]. The broad band at 930 cm^{-1} could be assigned to the V–O–V stretching in the bi-dimensional vanadia layer [36]. The band at about 1030 cm^{-1}, which is known to correspond to V=O stretching in the isolated VO_x species was not detected. These facts (which are also supported by TEM pictures in which no vanadium aggregates were observed) suggest that the polymeric vanadium oxide species were homogeneously dispersed over the Al_2O_3–TiO_2 support. Similar results were also obtained for the active phase of the catalytic membrane reactor.

Fig. 5 shows changes in the permeance behaviour between the prepared catalytic membranes and the respective starting ceramic tubes. For both the ATV and the ATVimp membranes the overall permeance decreased showing a lower permeance dependence on the average pressure than the starting ceramic tubes, which demonstrated a remarkable contribution of Poiseuille to the overall permeance.

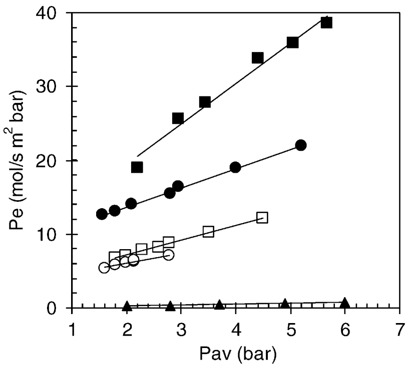

Fig. 5. Helium permeance against the average pressure for the α-$Al_2O_3$200 nm support (■), Atech 20kD (●), ATV (□), the ATVimp (○) membranes and the SiO_2 membrane (▲).

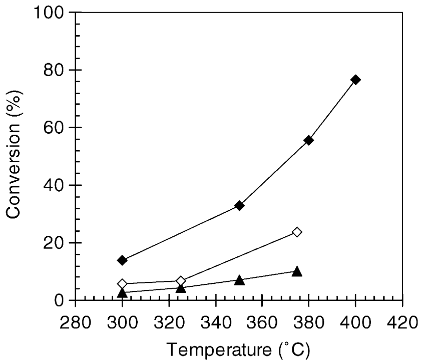

Fig. 6. Toluene conversion towards the reaction temperature for the (◆) packed bed reactor and the (◇) ATVimp and (▲) ATV catalytic membrane reactors.

The SiO_2 membrane had the lowest permeance (about 0.4 mol s^{-1} m^{-2} bar^{-1}) with a predominant Knudsen transport regime (the permeance was practically independent on the average pressure).

3.2. Reaction results

Fig. 6 compares the conversion-temperature trends for the PBR and CMRs. These trends were obtained by varying the temperature between 300 and 400 °C. The packed bed membrane reactor reached higher toluene conversions than the CMRs due to the very different amount of catalytic phase present in the two systems.

The mean residence time of reactants, τ, is directly proportional to the catalyst amount in the reactor when all the other operating conditions are fixed. Therefore, in our experimental conditions

$$\tau_{\text{packed-bed}} : \tau_{\text{ATVimp}} : \tau_{\text{ATV}} = W_{\text{packed-bed}} : W_{\text{ATVimp}} : W_{\text{ATV}} \approx 14 : 2 : 1$$

where W_i is the vanadium amount in the reactor.

For the PBR and ATVimp CMR, the selectivity toward the useful products (benzaldehyde and benzoic acid) was higher at the lowest temperature studied (300 °C) and reached a value of about 80%. When the temperature was increased up to 400 °C the benzoic acid and benzaldehyde dramatically decreased, while CO_2 selectivity increased and CO also appeared over 370 °C for high toluene conversion levels.

For the ATV membrane the mean residence time of toluene and its intermediate products was very low and over oxidation, which formed carbon oxides, was minimised being always smaller than 15%.

For the PBR two different O_2/T ratios were investigated. The results are reported in terms of product yield at various temperatures in Table 2. The O_2/T ratio influenced more the toluene conversion rather than the intermediate products selectivity, with a higher benzoic acid yield for higher O_2/T ratios. Moreover, at the highest O_2/T ratio the CO_2 yield

Table 2
Effect of the O_2/T ratio on the performance of the $V/Al_2O_3–TiO_2$ catalyst in a packed bed reactor

O_2/T	Temperature (°C)	Conversion (%)	Yield (%)		
			Benzaldehyde	Benzoic acid	Carbon dioxide
5	300	20.9	2.3	18.5	0.2
	325	22.8	3.1	19.2	0.5
	350	23.5	4.1	18.4	1.0
	375	25.5	5.2	17.8	2.5
	400	48.4	4.3	15.5	5.6
12	325	29.8	3.1	25.4	1.3
	350	38.0	5.0	29.4	3.6
	380	55.5	3.4	29.6	9.3
	400	76.7	2.4	23.8	18.0

increased greatly, revealing the consecutive character of the combustion reaction with respect to the reaction that leads to benzoic acid.

3.3. Feed configuration

Fig. 7 reports the selectivity-conversion behaviour at two different temperatures for the monolith-like and the flow-through modes in the ATV catalytic membrane. At both the studied temperatures the selectivity was practically constant and no differences were observed between the two feed configurations tested. In the ATV catalytic membrane the catalytic phase was arranged as a very thin mesoporous layer. The catalyst was both efficiently and completely used in the two configurations and as mentioned before, this membrane had the lowest residence time when compared to the other reactor arrangements.

Fig. 8 shows the effect of different contact modes on the performance of the ATVimp catalytic membrane reactor. In the ATVimp catalytic membrane reactor the various feeding policies changed the selectivity of the main intermediate product (benzaldehyde). The flow-through configuration gave a lower benzaldehyde selectivity than the other two configurations. The best feed contact mode was the mixed-flow mode with a benzaldehyde selectivity of about 76% at the lower toluene conversion value (6%). In the ATVimp membrane the catalytic phase $V/Al_2O_3–TiO_2$ was distributed along the catalytic membrane cross-section. The performance of this type of catalytic membrane reactor is linked to the amount of catalyst and distribution profile along the membrane cross-section. The back permeation of toluene and intermediate products is avoided by externally feeding oxygen and He (mixed-flow mode) and then the consecutive reactions of combustion were minimised [20]. The flow-through configuration improves the contact between the reactants and the catalyst especially when the catalytic membranes work in the Knudsen regime [37]. The reactant profiles across the membrane section were more favourable in the mixed-flow mode than in the other two (flow-through and monolith-like modes) since the wider reaction zone present in this type of catalytic membrane reactor better exploited these profiles.

The influence of the feeding modes on the performance of the inert membrane reactor are reported in Fig. 9 as a function of the O_2/T molar ratio. The mixed-feed configuration compared with the co-feed configuration did not improve the selectivity. Probably an inert membrane with a lower oxygen permeance would further improve the selectivity to intermediate compounds as found by Ramos et al. [19] who increased the selectivity to propylene (reaction of oxidehydrogenation of propane) by about

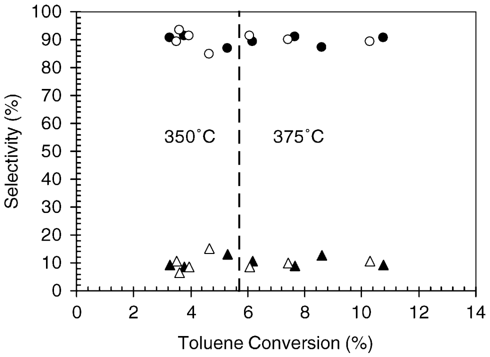

Fig. 7. Benzaldehyde (circles) and CO_2 (triangles) selectivity for the ATV catalytic membrane reactor working in the (filled symbols) monolith-like of (empty symbols) flow-through modes.

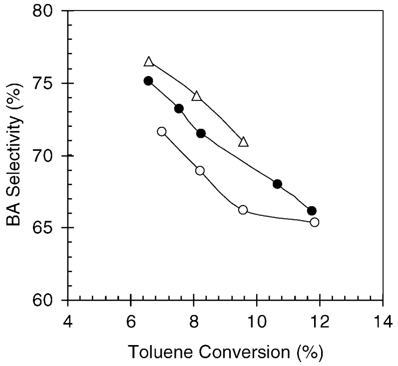

Fig. 8. Benzaldehyde selectivity vs. toluene conversion for the ATVimp catalytic membrane reactor working in the (△) mixed flow, (●) monolith flow, (○) and flow-through modes. O_2/T between 9 and 40. Temperature = 350 °C and flowrate = 60 cm^3/min.

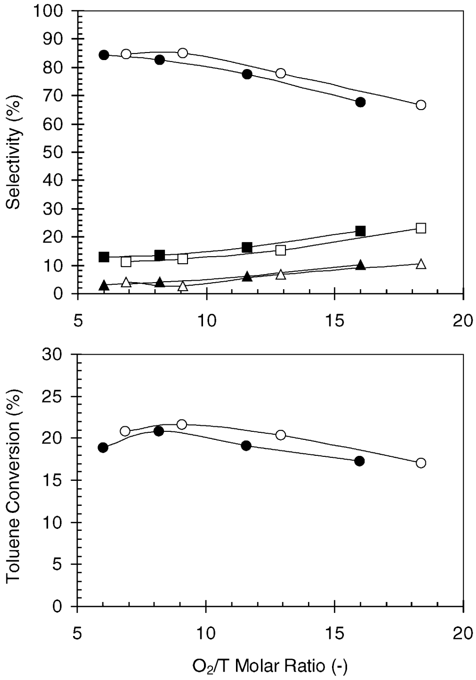

Fig. 9. The co-feed (full symbols) against mixed-feed (empty symbols) configurations for the inert membrane reactor at various O_2/T molar ratio. In the above figure: (circles) benzoic acid, (square) benzaldehyde and (triangles) CO_2 selectivities. $T = 325\ ^{\circ}C$, total flowrate = 77 cm^3/min.

5–10% at a fixed conversion by lowering the membrane permeance. In this sense further investigations are in progress.

4. Conclusions

The catalyst, $V/Al_2O_3–TiO_2$, gave interesting selective oxidation of toluene to benzoic acid and benzaldehyde. The support was developed using the sol–gel technique and procedure of vanadium deposition allowed for avoiding the presence of bulk V_2O_5. High benzoic acid selectivity was obtained in the PBR. When toluene conversion was lower than 15%, high benzaldehyde selectivity was obtained with the $V/Al_2O_3–TiO_2$ catalytic membranes. The CMR was able to further improve the selectivity of the main intermediate product of the process by using both an opportune feeding configuration and a particular catalyst distribution along the membrane cross-section. The IMPBR poorly improved the benzoic acid selectivity with respect to the PBR. This should be pursued by preparing inert membranes with a suitable oxygen permeability.

Acknowledgements

The financial support of MIUR (PRIN) is acknowledged. We would also like to thank Dr. E. Aghemo for the experimental support.

References

[1] B. Grzybowska-Swierkosz, Appl. Catal. 157 (1997) 263.
[2] T. Maki, Y. Suzuki, Benzoic acid and derivatives, in: Ullmann's Encyclopedia of Industrial Chemistry, vol. A3, Wiley–VCH, New York, 1985.
[3] A. Martin, B. Lucke, Catal. Today 57 (2000) 61.
[4] M. Ponzi, C. Duschatzky, A. Carrascul, E. Ponzi, Appl. Catal. A 169 (1998) 373.
[5] B. Jonson, B. Rebenstorf, R. Larsson, S.L.T. Andersson, J. Chem. Soc., Faraday Trans. 84 (1988) 3547.
[6] D.A. Bulushev, L. Kiwi-Minsker, A. Renken, Catal. Today 57 (2000) 231.
[7] J. Zhu, S.L.T. Andersson, J. Chem. Soc., Faraday Trans. 85 (1989) 3629.
[8] J. Zhu, D. Rebenstorf, S.L.T. Andersson, Faraday Trans. 85 (1989) 3645.
[9] D.A. Bulushev, F. Rainone, L. Kiwi-Minsker, A. Renken, Langmuir 17 (2001) 5276.
[10] H.K. Matralis, Ch. Papadopoulou, Ch. Kordulis, A. Aguilar Elguezabal, V. Cortes Corberan, Appl. Catal. A 126 (1995) 365.
[11] D.A. Bulushev, L. Kiwi-Minsker, V.I. Zaikovskii, O.B. Lapina, A.A. Ivanov, S.I. Reshetnikov, A. Renken, Appl. Catal. A 202 (2000) 243.
[12] S. Larrondo, B. Firigoyen, G. Baronetti, N. Amadeo, Appl. Catal. A 250 (2003) 279.
[13] B.M. Weckhuysen, D.E. Keller, Catal. Today 78 (2003) 25.
[14] F. Rainone, L. Kiwi-Minsker, D.A. Bulushev, P.A. Buffat, A. Renken, Appl. Catal. A 244 (2003) 251.
[15] P. Kölsch, M. Noack, R. Schäfer, G. Georgi, R. Omorjan, J. Caro, J. Mem. Sci. 198 (2002) 119.
[16] J. Coronas, M. Menendez, J. Santamaria, Ind. Eng. Chem. Res. 34 (1995) 4229.
[17] A. Pantazidis, J.A. Dalmon, C. Mirodatos, Catal. Today 25 (1995) 403.
[18] C. Tellez, M. Menendez, J. Santamaria, AIChE J. 43 (1997) 777.
[19] R. Ramos, M. Menendez, J. Santamaria, Catal. Today 56 (2000) 239.
[20] M.J. Alfonso, M. Menendez, J. Santamaria, Chem. Eng. J. 90 (2002) 131.
[21] M.J. Alfonso, M. Menendez, J. Santamaria, Catal. Today 56 (2000) 247.
[22] F. Klose, T. Wolf, S. Thomas, A. Seidel-Morgensten, Appl. Catal. A 257 (2004) 193.
[23] A. Bottino, G. Capannelli, A. Comite, J. Mem. Sci. 197 (2002) 75.
[24] S. Mota, S. Miadron, J.-C. Volta, J.-A. Dalmon, Catal. Today 67 (2001) 169.
[25] R. Mallada, M. Menendez, J. Santamaria, Catal. Today 56 (2000) 191.
[26] E. Xue, J. Ross, Catal. Today 61 (2000) 3.
[27] S. Agarwalla, C.R.F. Lund, J. Mem. Sci. 70 (1992) 129.
[28] G. Saracco, V. Specchia, Catal. Rev. Sci. Eng. 36 (1994) 305.
[29] J. Coronas, M. Menendez, J. Santamaria, Loss Prev. Process Ind. 8 (1995) 97.
[30] A. Bottino, G. Capannelli, F. Cerutti, A. Comite, R. Di Felice, Chem. Eng. Res. Des. 82 (2004) 229.
[31] E. Bergaglio, A. Bottino, A. Comite, G. Capannelli, J. Mem. Sci., in preparation.
[32] A. Larbot, A. Julbe, C. Guizard, L. Cot, J. Mem. Sci. 44 (1989) 289.
[33] G. Vitulli, E. Pitzalis, P. Salvadori, G. Capannelli, O. Monticelli, A. Servida, A. Julbe, Catal. Today 25 (1995) 249.
[34] W.F. Zhang, Y.L. He, M.S. Zhang, Z. Yin, Q. Chen, J. Phys. D: Appl. Phys. 33 (2000) 912.
[35] S.-H. Lee, H.M. Cheong, M.J. Seong, P. Liu, C.E. Tracy, A. Mascarenhas, J.R. Pitts, S.K. Deb, Solid State Ionics 165 (2003) 111.
[36] G.T. Went, L.-J. Leu, A.T. Bell, J. Catal. 134 (1992) 479.
[37] M. Gonzalez-Burillo, A.L. Barbosa, J. Herguido, J. Santamaria, J. Catal. 218 (2003) 457.